

Original Article

A rhesus monkey model of common carotid stenosis

Ziming Ye^{1*}, Ying Liu^{2*}, Xiawei Wang¹, Xiangren Chen¹, Cuiting Lin¹, Ying Su¹, Tianbao Wang¹, Yanyan Tang¹, Yuan Wu¹, Chao Qin¹

¹Department of Neurology, The First Affiliated Hospital, Guangxi Medical University, Nanning, Guangxi, P. R. China; ²Department of Rehabilitation Medicine, The First Affiliated Hospital, Guangxi Medical University, Nanning, Guangxi, P. R. China. *Equal contributors.

Received January 21, 2016; Accepted August 4, 2016; Epub September 15, 2016; Published September 30, 2016

Abstract: Objective: There are no common carotid stenosis (CCS) models in non-human primate animals yet. In this study, we combined the balloon injury in the left common carotid arteries (CCAs) with fat-rich feeding to establish a CCS model in the aged rhesus monkeys. Methods: Sixteen aged rhesus monkeys (14-18 years, 7.6-10.7 kg) were averagely allocated into the model and control groups, respectively. All the monkeys were made balloon injury in the left CCAs, and monkeys in the model and control groups received high-fat food and normal food, respectively. At baseline and 20 weeks after the operation, the body weight and serum levels of blood lipids were measured. CCS and hemodynamic changes of CCAs were detected by the ultrasound and digital subtraction angiography (DSA) examinations, respectively. Results: Twenty weeks later after the operation, the model group monkeys exhibited apparent CCS in the left CCAs with an average CCS extent of $44.99 \pm 3.93\%$, while the control group did not ($P < 0.001$). Significantly decreased arterial lumen diameter and increased systolic and diastolic peak velocity were observed in the model group relative to control group at 20 weeks as well as to model group at baseline (all $P < 0.05$). Furthermore, there was significant difference in mean transit time, time to peak, and time of appearance of peak value on DSA images between the model and control groups (all $P < 0.05$). Conclusions: The combination of balloon injury with fat-rich feeding for 20 weeks is feasible and effective for the preparation of a CCS model in the aged rhesus monkeys.

Keywords: Common carotid stenosis, common carotid arteries, model, rhesus monkey, balloon injury, high-fat

Introduction

Ischemic cerebrovascular disease (ICVD), characterized as high morbidity, mortality and recurrence rate [1, 2], becomes a heavy socioeconomic and psychological burden. Until now, however, there have no sufficient and effective treatment regimens for ICVD yet. Carotid stenosis (CS) is demonstrated to be crucial for the pathogenesis and development of ICVD [3] because of the resultant abnormal hemodynamics [4-6]. To comprehensively elaborate the mechanisms underlying the pathogenesis and development of ICVD, it is necessary to establish a close-to-authenticity animal model of human common CS (CCS).

Up to now, there have been some animal models (such as mouse, rabbit, canine and swine models) of CCS induced by means of the combination of mechanical injury and fat-rich feed-

ing. Mice are most commonly applied for CCS model because of the good genetic knowledge, homogeneity within strains, low cost, and convenient genetic modification [7-10]. However, due to the small size of mice, the murine model is difficult for the interventional operation and *in-vivo* neuroimaging evaluation of lesions. Moreover, the inconsistent existence of posterior communicating arteries in mice might lead to high outcome variability [10]. As to rabbits and canines, although they have no disadvantage of small size and thus might be used for *in vivo* imaging observation, high variations of cerebral vessels that would influence the consistence of the outcomes make rabbits and canines far from being used as the optimal animal model of CCS [11-14]. For swines, the big obstacle for CS modeling is the high incidence of sudden death [15, 16]. In addition, all the aforementioned animals shared limited homologous genes with the humans, making these

A common carotid stenosis model in rhesus monkey

animal models difficult in simulating the real pathophysiological development from CS to ICVD in humans.

The rhesus monkeys are very close to the humans because they share over three quarters of homogenous genes with humans and that their biological behaviors, histological features and physiological metabolism also resemble to the humans [17]. This makes rhesus monkeys well simulate the pathogenesis and development of human diseases. Monkeys as the advanced primates are likely to be the ideal animal model of CCS simulating the clinical features of CCS in the humans due to the advanced genetic knowledge, suitable size, and similar physical conditions and biochemical aspects to the humans.

In the present study, we explored the feasibility and effectiveness of the combination of balloon injury in common carotid artery (CCA) with fat-rich feeding in the establishment of a close-to-authenticity CCS model in aged rhesus monkeys that simulates pathophysiological changes in the humans. This study will provide the basis for the mechanism investigation as well as the related drug development of human CCS and ICVD.

Materials and methods

Animals

Sixteen male aged rhesus monkeys (14-18 years, 7.6-10.7 kg, Wincon Comp., Shantou, China) were used. All rhesus monkeys were labeled and housed in iron cages (one rhesus monkey per cage) with soft and warm bedding at the constant temperature (18-23°C) and humidity (50 ± 15%) under a 12-hour day/night cycle. Before the experiment, all monkeys were fed with the standard chow, including rice, flour, soya bean meal, fish meal, chicken meal, and soybean oil three times (100 gram chow for each time) daily, and freely got access to the tap water. The total 16 rhesus monkeys were averagely randomized into control group and model group, respectively, eight for each group. This study was approved by the Institutional Committee of Animal Care and Usage of Guangxi Medical University, Nanning, China.

Modeling procedures

All rhesus monkeys were made balloon injury in the middle segment of left CCA. Briefly, the

monkeys were placed and fixed in a supine position, with arms and legs fastened to the edges of the operating platform. Monkeys were sedated with intragluteal injection of atropine, induced anesthesia through intravenous injection of ketamine, and then maintained anesthesia through inhalation of 1.5% isoflurane. After that, monkeys received a tracheal intubation and were kept continuous ventilation via a special animal respirator (Harvard Model 683, Holliston Corp. Boston, USA). The rectal temperature (T) was monitored and maintained at 37°C by a CMA 50 feedback heating pad (Carnegie Medicine AB, Stockholm, Sweden). The vital signs (including pulse [P], heart rate [HR], respiration frequency [R] and blood pressure [BP]) and blood gas parameters (including the partial pressures of oxygen [PaO₂], carbon dioxide [PaCO₂], oxygen saturation [SaO₂], and arterial pH) were all monitored every ten minutes by means of a special vital sign monitor for animals (Wincon Comp.). Percutaneous arterial access through the Seldinger way was carried out via right femoral artery route and then a sheath was placed into this artery. With the help of steerable guide wires that were capable of getting across the femoral artery, a 5F MP-A1 guiding catheter (Evony, Cordis Corp., USA) was positioned into the proximal side of CCA. Then, the contrast agent Ultravist (Iopromide 370 Injection, Bayer Schering Pharma AG, Berlin, Germany) was injected 0.5 s later after the angiography onset to display the changes of vascular morphology and detect the occurrence of artery dissection and acute occlusion by both post-anterior-position and lateral-position carotid angiography using Siemens flat-panel digital cerebrovascular system (Axiom Artis Ece ceiling 146423, Siemens, Erlangen, Germany). The injecting velocity, flow, and maximal pressure of high-pressure injector were 3 ml/s, 6 ml, 150 pounds per square inch, respectively. The XR11 field was set to be 160 mm, while the diameter of output image was 180 mm. The distance between the X-ray tube and C-arm was 100 cm. The window width, window level and matrix of each image were set to be 4096, 2048 and 1024×1024, respectively.

With the help of carotid angiography, position of the 5F MP-A1 guiding catheter was deeply recorded so that it could be located 20 weeks later. After the first carotid angiography, balloon injury was made in the left CCA. The balloon was first calibrated well to make sure that the

A common carotid stenosis model in rhesus monkey

diameter ratio between the balloon and artery was 3:2, and was then located within easy reach for surgeons. Under the guidance of X-ray, a 5.0 mm×30 mm uninflated and compliant single-lumen balloon was slowly inserted into the middle segment of left CCA along with the aforementioned angiography pathway. After that, the balloon was appropriately inflated to a pre-determined pressure (6 atmospheres) and continuously pushed to make injury to the intima of CCA persisting for 30 s. Next, the balloon was deflated for 20 s and re-inflated 1 minute later. This procedure was carried out repeatedly for a total of three times, and finally the balloon was removed. Meanwhile, monkeys were prescribed with oral dual antiplatelet medications including 50 mg of clopidogrel hydrogen sulphate tablets (Plavix) and 50 mg of aspirin enteric-coated tablets (Bayaspirin) daily continuously for 3 days before the surgery and lasting for 14 days after the operation.

After the operation, the monkeys in the model group went on to be fed with a fat-rich chow which was made up of standard chow (60%), lard oil (30%) and refined sugar (10%) every day. For the control group, the monkeys similarly received the balloon injury in the left CCAs but were continuously fed with the normal standard chow every day after the operation.

CCS observation by digital subtraction angiography (DSA) measurement

Immediately after the balloon injury operation, monkeys received DSA examination in the left CCAs. One week after, monkey were checked if the arteries were occluded by color ultrasound examination (LOGIQ E9, General Electric, Fairfield, USA). Thereafter, color ultrasound examination was performed every 4 weeks. At 20 weeks after the operation, monkeys were re-checked by carotid DSA to make sure that both the 5F MP-A1-guided catheter and indexes of DSA imaging stayed the same position as previously determined by the first (before the balloon injury operation) and second (immediately after the operation) carotid angiography. The morphology of arteries was observed. Furthermore, based on the DSA imaging technique, the extent of CCS was evaluated according to the following formula [18]: stenosis = $[(A-B)/A] \times 100\%$, where A denoted for artery diameter of distal segment of CCS, while B for that of narrowest segment of CCS.

Hemodynamic observation by DSA imaging

Acquired original DSA images were processed and analyzed by Screenshots software and Photoshop 7.0 image processing software. The indexes of the post-anterior-position carotid angiography images were just abstracted and analyzed. Moreover, the regions of interest (ROIs) were set in the left CCA, brain tissue, and superior sagittal sinus. Of note, for the setting of the brain tissue ROI, areas of large blood vessels should be excluded as much as possible, and for the setting of the superior sagittal sinus ROI, areas of brain tissue should be ruled out as much as possible. DSA imaging data were processed by Photoshop 7.0 image processing software. K value (denoted for the density or grayscale of DSA images) of ROI was read. The K value of pure white area was defined as 0%, while that of pure black area was as 100%. Between them, the K value would increase with the increment of ROI darkness. The K value of ROI was read for three times. The mean K value and its corresponding acquisition time of a serial of DSA images within each rhesus monkey were then imported into the Microsoft Excel software (Version 2003) so as to obtain the curve of acquisition time-K value. Out from the curve, the indexes of DSA images, including peak value of the density (PV), mean transit time (MTT), time to peak (TP), and time of appearance of peak value (TAPV) were all abstracted for further analysis.

Ultrasound examination

To reduce the artifacts as possible, the left necks of monkeys were shaved and cleansed, and were then slightly extended along with the surface topography of CCA. Then monkeys were performed examination of color duplex sonography using an Agile ultrasound system (LOGIQ E9, General Electric, Fairfield, USA). The axial and lateral resolution was 0.5 mm and 0.45 mm, respectively; the transmitting and receiving frequency was set as 7.6 MHz, while the pulse repetition frequency was set as the maximal velocity without any aliasing. To decrease errors from false angle correction during the flow examinations, the angle correction was required to be below 60 degree and maintained all the same. The gain of this apparatus was adjusted to lower background noise in case of necessity. The characteristics of arteries such as lumen diameter (LD) were observed. The

A common carotid stenosis model in rhesus monkey

Table 1. Body weight and blood levels of lipids between the model and control groups

	Body weight	TC	TG	ApoA1	ApoB	HDL-C	LDL-C
Baseline							
Control group	9.09 ± 1.07	2.96 ± 0.34	0.61 ± 0.13	0.56 ± 0.07	0.33 ± 0.06	1.56 ± 0.21	1.25 ± 0.23
Model group	9.13 ± 1.01	2.94 ± 0.38	0.63 ± 0.17	0.57 ± 0.04	0.32 ± 0.05	1.53 ± 0.20	1.24 ± 0.32
P value	0.943	0.918	0.796	0.869	0.828	0.791	0.965
20 weeks							
Control group	8.70 ± 0.91	3.00 ± 0.34	0.62 ± 0.13	0.57 ± 0.10	0.33 ± 0.10	1.58 ± 0.21	1.27 ± 0.23
Model group	9.74 ± 0.63* [#]	3.50 ± 0.50* [#]	0.84 ± 0.11* [#]	0.57 ± 0.06	0.45 ± 0.07* [#]	1.52 ± 0.20	1.51 ± 0.21* [#]
P value	0.019	0.028	0.003	0.977	0.018	0.527	0.049

Abbreviations: TC, total cholesterol; TG, triglyceride; HDL-C, high density lipoprotein cholesterol; LDL-C, low density lipoprotein cholesterol; Apo-A1, apolipoprotein-A1; Apo-B, apolipoprotein-B. *P<0.05 compared with the model group at baseline, [#]P<0.05 compared with the control group at 20 weeks after the surgery.

pattern of velocity curve and related indexes of blood flow including systolic peak velocity (Vs) and diastolic peak velocity (Vd) were examined. These indexes were all measured at the sites of maximal stenosis or at the corresponding areas in CCAs.

Biochemical assessment

Blood samples were collected from the veins of left hind legs prior to and 20 weeks later after the modeling procedure. The serum levels of blood lipids, including total cholesterol (TC), triglyceride (TG), high density lipoprotein cholesterol (HDL-C), low density lipoprotein cholesterol (LDL-C), apolipoprotein-A1 (Apo-A1), and apolipoprotein-B (Apo-B) were measured according to the regular protocols of kits.

Behavioral observation

Prior to and 20 weeks later after the modeling procedure, the functions of nervous system in monkeys were comprehensively scored, including consciousness, sensation, movement, synchronization of skeletal muscle, and vision (bilateral) [19]. The score of 0 point represents a normal neural function, while 100-point represents a total abnormal neural function. Between them, the neural function becomes worse and worse with the increment of the scores [19].

Statistical analysis

All the quantitative data were normally distributed, expressed as mean ± standard derivation and statistically analyzed using SPSS 17.0 software for Windows (SPSS Inc., Chicago, IL, USA). Independent sample t test was used for appropriate comparison between the model and control groups at baseline and 20 weeks after the

operation, and paired t test was for the comparison between the data at baseline and at 20 weeks in both the two groups. P<0.05 was considered as statistical significance.

Results

General information of surgery

During the operation, the vital signs (including T, P, HR, R, and BP), and the blood gas parameters (including PaO₂, PaCO₂, SaO₂, and arterial pH) in monkeys were all kept normal. All monkeys responded well to the inhalation of isoflurane without any anesthetic side effects such as twitch, asphyxia, arrhythmia and respiratory depression. There were no rhesus monkeys died during and post the operation.

Body weight and blood levels of lipids

Through the pilot experiment for up to half a year, we determined the measurement before and at 20 weeks after the operation. Prior to the operation, there was no significant difference in the body weight and blood levels of lipids (TC, TG, HDL-C, LDL-C, Apo-A1, and Apo-B) between these two groups (all P>0.05, **Table 1**). Twenty weeks later, the body weight and blood levels of lipids in the control group almost remained unchanged (all P<0.05), while the body weight and blood levels of TC, TG, LDL-C and Apo-B in the model group were significantly increased compared with those at baseline (P<0.05) and were also significantly higher than those in the control group (all P<0.05, **Table 1**).

Neural behaviors

The neural behavioral scores remained 0 in all the monkeys both at baseline and 20 weeks after the operation, indicating that the model-

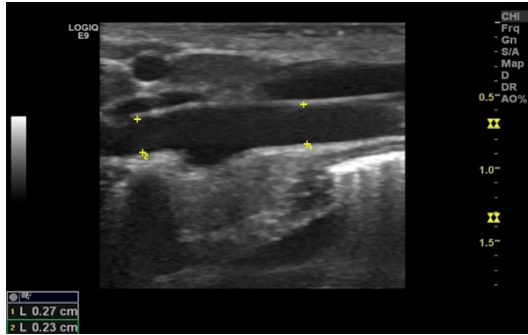


Figure 1. The arterial wall and lumen characteristics in a control group monkey after the balloon injury in the left CCA and 20-week normal feeding by ultrasound examination. Yellow labels were used to locate the measured arteries. The distance between upper and lower yellow labels was the diameter of artery (i.e. LD). The left lower frame showed the diameter of artery (i.e. 0.27 and 0.23 cm, respectively) at two different segments. L meant the left artery, and 1 and 2 represented 2 typical segments of the artery.

ing operation in this study did not influence the neural behaviors of monkeys.

Ultrasound examination

Prior to the operation, there was no CCS occurring in all the monkeys, and was no significant differences in LD, Vs, and Vd within the left CCAs between the two groups (all $P > 0.05$). Twenty weeks later, there was apparent narrowing and plaques in the left CCAs in the model group monkeys but without in the control group (**Figures 1 and 2**). The LD of the left CCAs was significantly smaller but the Vs and Vd were significantly higher in the model group than those in the control group at 20 weeks as well as than in the model group at baseline (all $P < 0.05$, **Table 2**). **Figures 2 and 3** showed the left CCA of a monkey within the model group manifested an apparent CS reflected by narrower lumen and faster blood flow.

DSA imaging

DSA examination showed that the left subclavian artery, left CCA and brachiocephalic trunk were all given off from the aorta, the left vertebral artery was from the left subclavian artery, while both the right CCA and subclavian arteries were from the brachiocephalic trunk. Besides, both the anterior and posterior communicating arteries were related to cerebral blood flow in the left and right sides. These results are consistent with the early study [20].

Twenty weeks later after the operation, DSA examination showed that the perfusion defect of contrast agent was observed in the left CCA of model group instead of control group (**Figures 4 and 5**), confirming the occurrence of CCS within the left CCA. The CCS extend was $44.99 \pm 3.93\%$ in the model group, a moderate CCS according to the NASCET criteria [18]. In contrast, no CS was observed in the control group ($P < 0.001$). Hemodynamic observation showed prior to the modeling procedures, there was no significant difference in PV, TP, TAPV, and MTT within CCA, brain tissue and superior sagittal sinus ROIs between the model and control groups (all $P > 0.05$). However, 20 weeks later, PV of CCA ROI was significantly lower but TP and TAPV were significantly higher in the model group than in the control group (all $P < 0.05$, **Table 3**). Since MTT was too short in CCA to exhibit accurate results during the measurement, it was only recorded in brain tissue and superior sagittal sinus ROIs but not in CCA ROI. Similarly, lower PV but higher TP, TAPV and MTT was observed in brain tissue and superior sagittal sinus ROIs of the model group compared with those of the control group (all $P < 0.05$, **Table 3**).

Discussion

This study demonstrated that through the balloon injury in the left CCA in combination with fat-rich feeding for 20 weeks, aged rhesus monkeys were induced characteristics of CCS as follows: 1) body weight and serum levels of lipids (including TC, TG, LDL-C and Apo-B) were significantly increased; 2) CCS was apparently observed in the left CCA by the ultrasound and DSA examinations; 3) ultrasound-based hemodynamic study showed that the LD of the left CCA was significantly decreased but the Vs and Vd were significantly increased; 4) DSA imaging-based hemodynamic study revealed that the TP, TAPV, and MTT were significantly increased, while PV was reduced. This established CCS model of aged rhesus monkeys was comprehensively confirmed through biochemical assessment, CCS determination (by ultrasound and DSA examinations), and hemodynamics study (by ultrasound and DSA examinations). Of note, DSA parameter imaging is a new special method for the confirmation of the CCS, which had not been previously reported. To our knowledge, this is the first report with regard to the establishment of CCS model in non-human pri-

A common carotid stenosis model in rhesus monkey

Table 2. Indexes of ultrasound observation between the model and control groups

	Baseline			20 weeks		
	LD (mm)	Vs (cm/s)	Vd (cm/s)	LD (mm)	Vs (cm/s)	Vd (cm/s)
Control group	3.49 ± 0.44	114.35 ± 6.97	30.10 ± 2.36	3.49 ± 0.46	115.11 ± 4.45	30.36 ± 4.15
Model group	3.51 ± 0.42	115.47 ± 4.01	30.60 ± 2.11	2.13 ± 0.45* [#]	121.84 ± 4.91* [#]	34.11 ± 1.81* [#]
P value	0.914	0.700	0.447	<0.001	0.012	0.035

Abbreviations: LD, lumen diameter; Vs, systolic peak velocity; Vd, diastolic peak velocity. *P<0.05 compared with the control group at 20 weeks after the surgery, [#]P<0.05 compared with the model group at baseline.

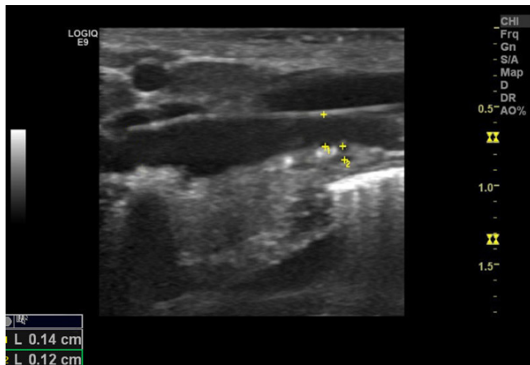


Figure 2. The arterial wall and lumen changes in a model group monkey after the balloon injury in the left CCA and 20-week fat-rich feeding by ultrasound examination. Yellow labels were used to locate the measured artery or plaque. The distance between upper and lower yellow labels was the diameter of artery (i.e. LD, shown as 1) and thickness of plaque (intima media thickness, shown as 2), respectively. The left lower frame showed the artery diameter of 0.14 cm (1 L) and the plaque thickness of 0.12 cm (2 L). L meant the left artery.

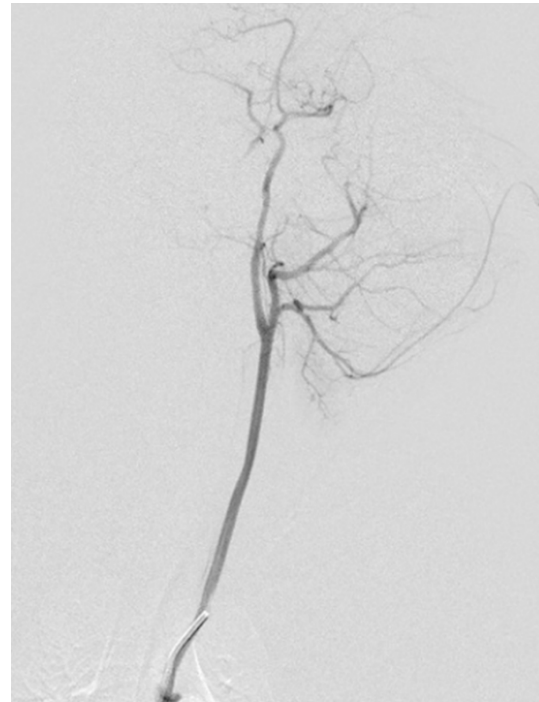


Figure 4. DSA observation of the left CCA in a control group monkey 20 weeks later after the operation. No stenosis was observed.

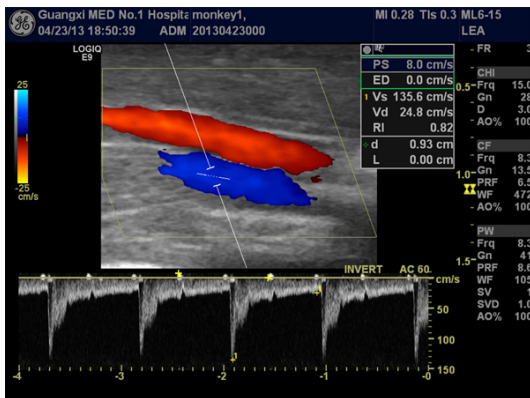


Figure 3. Hemodynamic changes in a model group monkey 20 weeks later after the operation by ultrasound examination. Red area showed the vein, and blue showed the artery. The Vs was measured to be 135.6 cm/s, and the Vd to be 24.8 cm/s.

mate animals. Since non-primate model is very similar to humans, this study will provide a

basis for the mechanism investigation of human CCS and ICVD, drug development, etc. Overweight or even obesity usually increases the risk of ICVD, especially ischemic stroke [21, 22]. Cholesterol and LDL are not only the mainly deposited components within arterial walls of atherosclerosis (AS), but also the inducers of inflammatory reactions and oxidative stress during the formation and development of AS [23, 24]. Therefore, both cholesterol and LDL are widely accepted as major risk factors of ICVD and as parameters for the diagnosis of ICVD as well. In addition, recent clinical investigations demonstrated that the serum levels of Apo-A1 and Apo-B are also associated with AS [25, 26]. We showed that body weight and serum levels of TC, TG, LDL-C and Apo-B were

A common carotid stenosis model in rhesus monkey

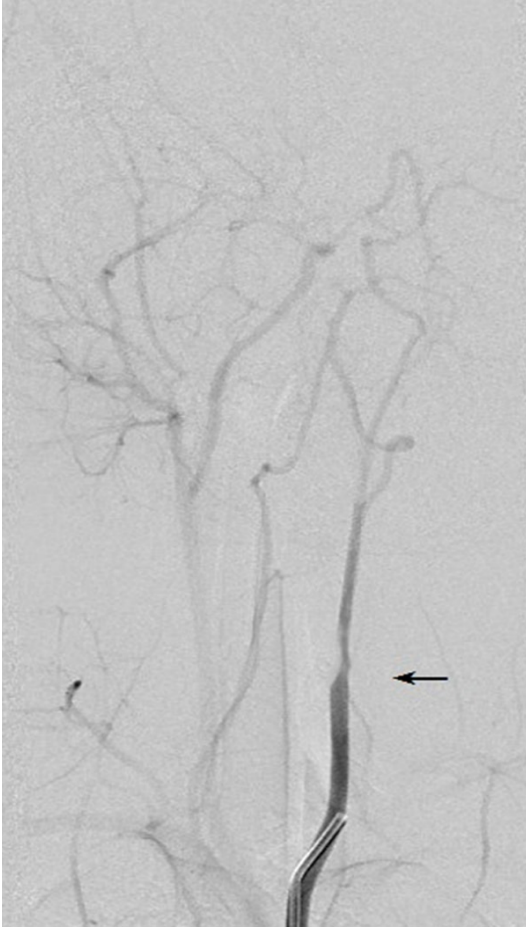


Figure 5. DSA observation of the left CCA in a model group monkey 20 weeks later after the operation. The narrow segment (arrowed) was clearly observed.

significantly elevated in rhesus monkeys receiving balloon injury and 20 weeks of fat-rich feeding, which is analogous to what happen to the humans suffering from CCS [27].

One of the most frequent outcomes caused by CCS is neural dysfunction [28]. Since the cerebral blood is mainly supplied by CCA system, CCS, especially severe CCS is usually bound to give rise to crucial neural outcomes [29, 30]. In the present study, we comprehensively evaluated the neural functions, including consciousness, sensation, movement, synchronization of skeletal muscle, and bilateral vision in the rhesus monkeys. Surprisingly, neural dysfunction at 20 weeks was not found in both the two groups, although up to $44.99 \pm 3.93\%$ CCS was observed in the left CCAs of the model group. This suggests that unilateral CCS does not always lead to irreversible ischemic injury to brain tissues and the consequently evident

manifestations of neural dysfunction. This might be attributable to the fact that collateral circulation of carotid arteries is more abundant within rhesus monkeys than that in the humans, and thus not all unilateral CS is likely to develop into ICVD with neural dysfunction in rhesus monkeys. The CCS monkey model in present study represents a moderate model that does not exhibit neural dysfunction. In fact, asymptomatic CCS without neural dysfunction is more frequent than symptomatic CCS with neural dysfunction. In addition, as a result of lack of special evaluation scales on neural functions for unilateral CCS, we have no choice but to apply a rapid evaluation scale for embolism in middle cerebral artery to our rhesus monkey model of unilateral CCS at present. In spite of being branched out from the CCA system, middle CCA supplies different brain areas from where are supplied by CCA. As a consequence, changes of neural functions caused by CCS of the left CCA may be inconsistent with that caused by stenosis of middle cerebral artery. This might be another reason why the neural functions were almost unchanged in all the monkeys throughout the experimental period.

As an *in-vivo* noninvasive neuroimaging method, ultrasound examination was used to evaluate the hemodynamic changes in CS models [16, 31]. However, ultrasound has low-quality resolution, difficulty in detecting coarse, irregular-shape and heterogeneous-textured objects such as the carotid arteries, and difficulty in exactly carrying out quantitative and qualitative representations of the found lesions. DSA is the gold standard of cerebral angiography that is used to evaluate hemodynamic changes after operation besides ultrasound examination. In this study, we combined the ultrasound with DSA examinations to determine the CCS in the CCAs of monkeys.

Plaques shown by ultrasound examination are likely to occur in arterial wall when the intima-media thickness (IMT) is in excess of 1.5 mm, which will lead to narrow lumen and fast blood flow. Even worse, plaques will also give rise to the follow-up development including rupture and ulceration, so that the distal end of artery is about to be occluded. Thickening of IMT and occurrence of plaques of the CCA are considered as effective indicators for the diagnosis of asymptomatic CS and prognosis of stroke risk [32-34]. Ultrasound examination in the present

A common carotid stenosis model in rhesus monkey

Table 3. DSA imaging acquisition indexes of CCA, brain tissue and superior sagittal sinus ROI between the model and control groups

	Control group	Model group	T	P
CCA ROI				
PV	16.64 ± 2.10	14.31 ± 1.45	2.579	0.022
TP	0.51 ± 0.0.12	0.65 ± 0.0.13	2.360	0.033
TAPV	0.89 ± 0.25	1.20 ± 0.26	2.196	0.032
Brain tissue ROI				
PV	2.81 ± 0.55	2.28 ± 0.34	2.300	0.037
TP	0.72 ± 0.11	0.95 ± 0.23	2.472	0.027
TAPV	1.69 ± 0.12	1.88 ± 0.17	2.432	0.029
MTT	1.47 ± 0.20	1.66 ± 0.14	2.175	0.047
Superior sagittal sinus ROI				
PV	43.70 ± 2.30	41.35 ± 1.15	2.584	0.022
TP	1.53 ± 0.27	1.78 ± 0.16	2.257	0.041
TAPV	2.97 ± 0.37	3.40 ± 0.38	2.327	0.035
MTT	1.57 ± 0.22	1.92 ± 0.36	2.357	0.034

Abbreviations: CCA, common carotid artery; PV, peak value of the density; TP, time to peak; TAPV, time of appearance of peak value; MTT, mean transit time.

study showed 20 weeks later after the modeling procedures, a few inhomogeneous-internal-echoes and convex to lumen plaques occurred in the balloon-injured area, and the thickened IMT and reduced LD were observed in the model group, indicating the appearance of CCS. DSA examination in this study showed that rhesus monkeys shared similar cerebral blood supply and anatomical orientation and distribution of cerebral vessels to those in humans, suggesting that the rhesus monkey is an optimal animal model for simulating the pathophysiological changes from CCS to ICVD in the humans. Further, DSA measurement verified the occurrence of CCS in the left CCAs simulating the CCS characteristics of the humans in aged rhesus monkeys after the operation of balloon injury in combination with 20-week of fat-rich feeding.

Hemodynamic change in CCA is an important feature of a success CCS model [16, 31], we thus observed the hemodynamic changes in the two group monkeys using ultrasound and DSA techniques, respectively. Ultrasound examination showed in addition to the thicken IMT and reduced LD of left CAAs, faster Vs and Vd were also observed in the model group. These characteristics were analogous to what have been verified in patients with CCS [35-37], suggesting that balloon injury in CCA plus fat-rich

feeding for 20 weeks can effectively induce the CCS. DSA is widely accepted for cerebral angiography and is also used as a new way to evaluate the hemodynamic changes [38]. With the development of computer techniques and processing softwares, DSA imaging is more and more being applied to evaluate the hemodynamic changes after arterial stenosis [39]. We showed that shorter PV but longer TP and TAPV in CCA ROI as well as shorter PV but longer TP, TAPV and MTT within both the brain tissue and superior sagittal sinus ROIs were all observed 20 weeks later after the modeling procedures in model group as compared with control group. This finding further indicates that significantly aberrant hemodynamic changes occur after CCS. The present study preliminarily demonstrates that the application of DSA imaging is feasible to evaluate the follow-up hemodynamic changes after CCS, which has not been previously reported.

An important limitation of this study is that for some reasons, monkeys were not sacrificed for histological analysis. However, ultrasound observation and DSA imaging evaluation confirmed the success of the establishment of CCS in aged rhesus monkeys.

Conclusions

The combination of balloon injury in the left CCA with fat-rich feeding is feasible and effective for the establishment of CCS model that simulates the characteristics of human CCS in the aged rhesus monkeys. This study will provide a basis for the mechanism investigation and the related drug development of human CCS and ICVD.

Acknowledgements

The present study was funded by the grant from National Nature Science Foundation of China (No. 81360191).

Disclosure of conflict of interest

None.

Address correspondence to: Dr. Chao Qin, Department of Neurology, The First Affiliated Hospital, Guangxi Medical University, Nanning 530-021, Guangxi, P. R. China. Tel: 86-0771-5356735; Fax: 86-0771-5350031; E-mail: mdqc6639@163.com

A common carotid stenosis model in rhesus monkey

References

- [1] Lopez AD, Mathers CD, Ezzati M, Jamison DT and Murray CJ. Global and regional burden of disease and risk factors, 2001: systematic analysis of population health data. *Lancet* 2006; 367: 1747-57.
- [2] Strong K, Mathers C and Bonita R. Preventing stroke: saving lives around the world. *Lancet Neurol* 2007; 6: 182-187.
- [3] Young KC, Jain A, Jain M, Replogle RE, Benesch CG and Jahromi BS. Evidence-based treatment of carotid artery stenosis. *Neurosurg Focus* 2011; 30: E2.
- [4] Mono ML, Karameshev A, Slotboom J, Remonda L, Galimanis A, Jung S, Findling O, De Marchis GM, Luedi R, Kiefer C, Stucker C, Mattle HP, Schroth G, Arnold M, Nedeltchev K and El-Koussy M. Plaque characteristics of asymptomatic carotid stenosis and risk of stroke. *Cerebrovasc Dis* 2012; 34: 343-50.
- [5] Merwick Á, Albers GW, Arsava EM, Ay H, Calvet D, Coutts SB, Cucchiara BL, Demchuk AM, Giles MF, Mas JL, Olivot JM, Purroy F, Rothwell PM, Saver JL, Sharma VK, Tsivgoulis G and Kelly PJ. Reduction in early stroke risk in carotid stenosis with transient ischemic attack associated with statin treatment. *Stroke* 2013; 44: 2814-20.
- [6] Marnane M, Prendeville S, McDonnell C, Noone I, Barry M, Crowe M, Mulligan N and Kelly PJ. Plaque inflammation and unstable morphology are associated with early stroke recurrence in symptomatic carotid stenosis. *Stroke* 2014; 45: 801-6.
- [7] Zhang L, Ya B, Yang P, Sun F, Zhang L, Li Y and Li L. Impact of carotid atherosclerosis combined with hypercholesterolemia on cerebral microvessels and brain parenchyma in a new complex rat model. *Neurochem Res* 2014; 39: 653-60.
- [8] Wicks RT, Huang Y, Zhang K, Zhao M, Tyler BM, Suk I, Hwang L, Ruzevick J, Jallo G, Brem H, Pradilla G and Kang JU. Extravascular optical coherence tomography: evaluation of carotid atherosclerosis and pravastatin therapy. *Stroke* 2014; 45: 1123-30.
- [9] Tao M, Mauro CR, Yu P, Favreau JT, Nguyen B, Gaudette GR and Ozaki CK. A simplified murine intimal hyperplasia model founded on a focal carotid stenosis. *Am J Pathol* 2013; 182: 277-87.
- [10] Zhen G and Doré S. Optimized protocol to reduce variable outcomes for the bilateral common carotid artery occlusion model in mice. *J Neurosci Methods* 2007; 166: 73-80.
- [11] Le Veen RF, Wolf GL and Villanueva TG. New rabbit atherosclerosis model for the investigation of transluminal angioplasty. *Invest Radiol* 1982; 17: 470-475.
- [12] Li R, Lan B, Zhu T, Yang Y, Wang M, Ma C and Chen S. Establishment of an animal model of vascular restenosis with bilateral carotid artery grafting. *Med Sci Monit* 2014; 20: 2846-54.
- [13] Zheng J, Chang Z, Hou Y, Liu Z, Lu Z, Guo Q and Li X. Accuracy of MDCT for detection and identification of carotid atherosclerotic plaque in a rabbit model. *AJR Am J Roentgenol* 2014; 202: W176-81.
- [14] Calderon-Arnulphi M, Amin-Hanjani S, Alaraj A, Zhao M, Du X, Ruland S, Zhou XJ, Thulborn KR and Charbel FT. In vivo evaluation of quantitative MR angiography in a canine carotid artery stenosis model. *AJNR Am J Neuroradiol* 2011; 32: 1552-9.
- [15] Klein AJ, Tomkowiak MT, Vigen KK, Hacker TA, Speidel MA, Vanlysel MS, Shah N and Raval AN. Multimodality image fusion to guide peripheral artery chronic total arterial occlusion recanalization in a swine carotid artery occlusion model: unblinding the interventionalist. *Catheter Cardiovasc Interv* 2012; 80: 1090-8.
- [16] Soulez G, Lerouge S, Allard L, Roméo P, Qi S, Héon H, Tardif JC and Cloutier G. Vulnerable carotid atherosclerotic plaque creation in a Swine model: evaluation of stenosis creation using absorbable and permanent suture in a diabetic dyslipidemic model. *J Vasc Interv Radiol* 2012; 23: 1700-1708, e4.
- [17] Rhesus Macaque Genome Sequencing and Analysis Consortium, Gibbs RA, Rogers J, Katze MG, Bumgarner R, Weinstock GM, Mardis ER, Remington KA, Strausberg RL, Venter JC, Wilson RK, Batzer MA, Bustamante CD, Eichler EE, Hahn MW, Hardison RC, Makova KD, Miller W, Milosavljevic A, Palermo RE, Siepel A, Sikela JM, Attaway T, Bell S, Bernard KE, Buhay CJ, Chandrabose MN, Dao M, Davis C, Delehaunty KD, Ding Y, Dinh HH, Dugan-Rocha S, Fulton LA, Gabisi RA, Garner TT, Godfrey J, Hawes AC, Hernandez J, Hines S, Holder M, Hume J, Jhangiani SN, Joshi V, Khan ZM, Kirkness EF, Cree A, Fowler RG, Lee S, Lewis LR, Li Z, Liu YS, Moore SM, Muzny D, Nazareth LV, Ngo DN, Okwuonu GO, Pai G, Parker D, Paul HA, Pfannkoch C, Pohl CS, Rogers YH, Ruiz SJ, Sabo A, Santibanez J, Schneider BW, Smith SM, Sodergren E, Svatek AF, Utterback TR, Vattathil S, Warren W, White CS, Chinwalla AT, Feng Y, Halpern AL, Hillier LW, Huang X, Minx P, Nelson JO, Pepin KH, Qin X, Sutton GG, Venter E, Walenz BP, Wallis JW, Worley KC, Yang SP, Jones SM, Marra MA, Rocchi M, Schein JE, Baertsch R, Clarke L, Csürös M, Glasscock J, Harris RA, Havlak P, Jackson AR, Jiang H, Liu Y, Messina DN, Shen Y, Song HX, Wylie T, Zhang L, Birney E, Han K, Konkel MK, Lee J, Smit AF, Ullmer B, Wang H, Xing J, Burhans R, Cheng Z, Karro JE, Ma J, Raney B, She X, Cox MJ, Demuth JP, Dumas LJ, Han SG, Hopkins J, Karimpour-Fard A, Kim YH,

A common carotid stenosis model in rhesus monkey

- Pollack JR, Vinar T, Addo-Quaye C, Degenhardt J, Denby A, Hubisz MJ, Indap A, Kosiol C, Lahn BT, Lawson HA, Marklein A, Nielsen R, Vallender EJ, Clark AG, Ferguson B, Hernandez RD, Hirani K, Kehrer-Sawatzki H, Kolb J, Patil S, Pu LL, Ren Y, Smith DG, Wheeler DA, Schenck I, Ball EV, Chen R, Cooper DN, Giardine B, Hsu F, Kent WJ, Lesk A, Nelson DL, O'brien WE, Prüfer K, Stenson PD, Wallace JC, Ke H, Liu XM, Wang P, Xiang AP, Yang F, Barber GP, Haussler D, Karolchik D, Kern AD, Kuhn RM, Smith KE and Zwiag AS. Evolutionary and biomedical insights from the rhesus macaque genome. *Science* 2007; 316: 222-34.
- [18] Gasecki AP, Eliasziw M, Ferguson GG, Hachinski V and Barnett HJ. Long-term prognosis and effect of endarterectomy in patients with symptomatic severe carotid stenosis and contralateral carotid stenosis or occlusion: results from NASCET. North American Symptomatic Carotid Endarterectomy Trial (NASCET) Group. *J Neurosurg* 1995; 83: 778-82.
- [19] Kito G, Nishimura A, Susumu T, Nagata R, Kuge Y, Yokota C and Minematsu K. Experimental thromboembolic stroke in cynomolgus monkey. *J Neurosci Methods* 2001; 105: 45-53.
- [20] Ryan KG, Simeone FA, Cortese DA and Cotter JR. Cerebral angiography in the Rhesus monkey. *Invest Radiol* 1969; 4: 34-40.
- [21] Global Burden of Metabolic Risk Factors for Chronic Diseases Collaboration (BMI Mediated Effects), Lu Y, Hajifathalian K, Ezzati M, Woodward M, Rimm EB and Danaei G. Metabolic mediators of the effects of body-mass index, overweight, and obesity on coronary heart disease and stroke: a pooled analysis of 97 prospective cohorts with 1.8 million participants. *Lancet* 2014; 383: 970-83.
- [22] Doehner W, Schenkel J, Anker SD, Springer J and Audebert HJ. Overweight and obesity are associated with improved survival, functional outcome and stroke recurrence after acute stroke or transient ischaemic attack: observations from the TEMPIS trial. *Eur Heart J* 2013; 34: 268-277.
- [23] Staprans I, Pan XM, Rapp JH and Feingold KR. The role of dietary oxidized cholesterol and oxidized fatty acids in the development of atherosclerosis. *Mol Nutr Food Res* 2005; 49: 1075-1082.
- [24] Mitra S, Goyal T and Mehta JL. Oxidized LDL, LOX-1 and atherosclerosis. *Cardiovasc Drugs Ther* 2011; 25: 419-429.
- [25] Paultre F, Tuck CH, Boden-Albala B, Kargman DE, Todd E, Jones J, Paik MC, Sacco RL and Berglund L. Relation of Apo(a) size to carotid atherosclerosis in an elderly multiethnic population. *Arterioscler Thromb Vasc Biol* 2002; 22: 141-6.
- [26] Walldius G, Jungner I, Holme I, Aastveit AH, Kolar W and Steiner E. High apolipoprotein B, low apolipoprotein A-I, and improvement in the prediction of fatal myocardial infarction (AMORIS study): a prospective study. *Lancet* 2001; 358: 2026-33.
- [27] Chróinin DN, Marnane M, Akijian L, Merwick A, Fallon E, Horgan G, Dolan E, Murphy S, O'Rourke K, O'Malley K, O'Donohoe M, McDonnell C, Noone I, Barry M, Crowe M, Kavanagh E, O'Connell M and Kelly PJ. Serum lipids associated with inflammation-related PET-FDG uptake in symptomatic carotid plaque. *Neurology* 2014; 82: 1693-9.
- [28] Avirame K, Lesemann A, List J, Witte AV, Schreiber SJ and Flöel A. Cerebral autoregulation and brain networks in occlusive processes of the internal carotid artery. *J Cereb Blood Flow Metab* 2015; 35: 240-7.
- [29] Marnane M, Prendeville S, McDonnell C, Noone I, Barry M, Crowe M, Mulligan N and Kelly PJ. Plaque inflammation and unstable morphology are associated with early stroke recurrence in symptomatic carotid stenosis. *Stroke* 2014; 45: 801-6.
- [30] Mono ML, Karameshev A, Slotboom J, Remonda L, Galimanis A, Jung S, Findling O, De Marchis GM, Luedi R, Kiefer C, Stuker C, Mattle HP, Schroth G, Arnold M, Nedelchev K and El-Koussy M. Plaque characteristics of asymptomatic carotid stenosis and risk of stroke. *Cerebrovasc Dis* 2012; 34: 343-50.
- [31] Hölscher T, Ahadi G, Fisher D, Zadicario E and Voie A. MR-guided focused ultrasound for acute stroke: a rabbit model. *Stroke* 2013; 44 Suppl 1: S58-60.
- [32] Harloff A, Strecker C, Reinhard M, Kollum M, Handke M, Olschewski M, Weiller C and Hetzel A. Combined measurement of carotid stiffness and intima-media thickness improves prediction of complex aortic plaques in patients with ischemic stroke. *Stroke* 2006; 37: 2708-12.
- [33] Elbaz A, Ripert M, Tavernier B, Février B, Zureik M, Gariépy J, Alperovitch A and Tzourio C. Common carotid artery intima-media thickness, carotid plaques, and walking speed. *Stroke* 2005; 36: 2198-202.
- [34] Touboul PJ, Labreuche J, Vicaut E, Amarenco P and GENIC Investigators. Carotid intima-media thickness, plaques, and Framingham risk score as independent determinants of stroke risk. *Stroke* 2005; 36: 1741-5.
- [35] Matos JM, Barshes NR, McCoy S, Pisimisis G, Felkai D, Kougas P, Lin PH and Bechara CF. Validating common carotid stenosis by duplex ultrasound with carotid angiogram or computed tomography scan. *J Vasc Surg* 2014; 59: 435-9.
- [36] Braun RM, Bertino RE, Milbrandt J, Bray M and Society of Radiologists in Ultrasound Consen-

A common carotid stenosis model in rhesus monkey

- sus Criteria to a Single Institution Clinical Practice. Ultrasound imaging of carotid artery stenosis: application of the Society of Radiologists in Ultrasound Consensus Criteria to a Single Institution Clinical Practice. *Ultrasound Q* 2008; 24: 161-6.
- [37] Grant EG, Benson CB, Moneta GL, Alexandrov AV, Baker JD, Bluth EI, Carroll BA, Eliasziw M, Gocke J, Hertzberg BS, Katanick S, Needleman L, Pellerito J, Polak JF, Rholl KS, Wooster DL and Zierler RE. Carotid artery stenosis: gray-scale and Doppler US diagnosis—Society of Radiologists in Ultrasound Consensus Conference. *Radiology* 2003; 229: 340-6.
- [38] Bürsch JH. Use of digitized functional angiography to evaluate arterial blood flow. *Cardiovasc Intervent Radiol* 1983; 6: 303-310.
- [39] Lin CJ, Chang FC, Guo WY, Hung SC, Luo CB, Beilner J, Kowarschik M and Chu WF. Changes of time-attenuation curve blood flow parameters in patients with and without carotid stenosis. *AJNR Am J Neuroradiol* 2015; 36: 1176-81.